Controlling Length and Monitoring Growth of Gold Nanorods

Hao-Ming Chen (陳浩銘) and Ru-Shi Liu* (劉如熹)
Department of Chemistry, National Taiwan University, Taipei 106, Taiwan, R.O.C.

In this paper, we report a new approach, which could fabricate gold nanowires by controlling the volume of growth solution. The shape evolutions ranging from fusiform nanoparticles to 1-D rods was observed. Increasing the addition of growth solution can control the length of nanorods. The length of rods can be extended to 2 μm, and nanorods with aspect ratios of up to ~ 70 could be obtained. Moreover, X-ray absorption spectroscopy (XAS) is applied herein to elucidate the growth mechanism of gold nanorods. The gold ions were directly reduced to gold atoms by ascorbic acid during the reaction, and then gold atoms were deposited on the surface of gold seeds that were introduced into the reaction. Extended X-ray absorption fine structure (EXAFS) confirmed the growth of gold and the environment around Au atoms over the reaction. The XAS are expected to have wide applications in the growth of gold and other related materials.

Keywords: Gold nanorods; X-ray absorption spectroscopy; Extended X-ray absorption fine structure.

INTRODUCTION

Several characteristics of nano-materials depend on size and shape, including their catalytic, optical and physical characteristics.[1-3] Spherical particles can be prepared easily by wet chemical methods. Anisotropic metal nanoparticles have been prepared using electrochemical means,[2] photochemical reduction in an aqueous system,[4] bubbling hydrogen with capping polymer,[5] and the polyol process.[6] Au nanorods with a small aspect ratio are of particular interest because of their optical properties. They exhibit transverse and longitudinal plasmon bands in the visible region of the spectrum, making them applicable in sensing and imaging fields.[7] 1-D nanoparticles can be prepared using templates that constrain the direction of growth of the crystal. Various chemical methods have been actively investigated to process metal into 1-D nanostructures.[8] Gold nanorods have been synthesized by electrochemical reduction in the presence of cetyltrmethylammonium bromide (CTAB)[9] and by seed-mediated growth in a surfactant template.[3]

More recently, the electrochemical method and seed-mediated growth method have been used with CTAB as the soft template, demonstrating the fabrication of gold nanorods dispersed in aqueous solution. The growth mechanism of 1-D gold nanoparticles in the presence of CTAB has been extensively examined.[11-15] The direction of growth of gold nanorods has been confirmed by analyzing the electron diffraction pattern and transmission electron microscopy (TEM) images.[10] Busbee et al. investigated the pH conditions of ascorbic acid for synthesizing gold nanorods.[11] The ascorbate monoanion over the acid or dianion increased the aspect ratio of the nanorods. Murphy et al. studied the concentration of silver ions, the $[Au^{3+}]$/[ascorbic acid] ratio, and the concentration of CTAB.[12,13] Branch Au nanoparticles, including tetra-pods, star-shaped nanoparticles and multi-pods, can be prepared at various [seed]/$[Au^{3+}]$ ratios. The surface structure of gold nanorods capped with cationic surfactants was investigated by IR. The results reveal the formation of a new bond, which shows the binding of the surfactant headgroups to the surface of nanorods.[14] Additionally, various surfactants such as alkyltrimethylammonium bromides and cetylpyridinium chloride have been investigated to use in synthesizing gold nanorods.[15] The results demonstrate that the aspect ratio of the resulting gold nanorods increased with the length of the surfactant chain. The surfactant binds as a bilayer to the growing nanorods and promotes the elongation of the nanorods via a "zipping" mechanism. Moreover, multifield ^2H relaxation has been used to quantify the effect of solu-

Dedicated to the memory of the late Professor Ho Tong-Ing.

* Corresponding author. E-mail: rsliu@ntu.edu.tw

bilization of alkanes on the size and shape of the micelles in aqueous solutions of hexadecyltrimethylammonium bromide, C_{16}TAB.[16] Recently we described a new approach, based on the seed-mediated method, which could extend the length of the resultant products using a simple procedure.[17] The local structures of nanomaterials are greatly important for future applications. Although TEM has been shown to be a powerful tool for the analysis of nanoparticles, it is limited to studying the chemical bonds and structural characteristics of multicomponent materials. However, X-ray absorption spectroscopy (XAS) can provide information about the nanostructure (e.g., coordination number, interatomic distance, and oxidation state of absorption atoms). This structural information is averaged over all of the X-ray-excited atoms in the entire sample, because a large percentage of the atoms in nanoparticles are at the interface. Extended X-ray absorption fine structure (EXAFS) was useful for identifying the random or preferred occupation of sites around specific atoms, and many studies about nanostructural analysis have been reported using EXAFS.[18-22] Thus, the local structures of gold nano wires were demonstrated in the present study.

EXPERIMENTAL SECTION

Preparation of Growth Solution

First, a 100 mL of 250 μM $HAuCl_4$ aqueous solution was prepared in a conical flask and then 3.0 g of solid CTAB was added to the gold salt solution. The solution was heated to 60 °C while stirring to dissolve the CTAB. The solution was used as the growth solution after cooling to room temperature.

Preparation of Gold Seeds

First, a 20 mL aqueous solution containing 0.25 mM $HAuCl_4$ and 0.25 mM trisodium citrate was prepared. Next, 0.6 mL of a 0.01 M $NaBH_4$ solution was added at once into the gold solution under constant stirring. Stirring was continued for another 30 s. The solution turned a wine red color indicating particle formation.

Growth of Rods

First, 0.02 mL of gold seeds was placed in a beaker. Then 0.2, 20, and 200 mL of growth solution were prepared. 0.1, 1, and 10 mL of freshly prepared ascorbic acid (AA; 10 mM) was mixed with each set, respectively. Next three colorless growth solutions were added to gold seeds solution per 1 min in order. The color of the solutions turned pink to violet within 10 min.

TEM images were acquired with a JEOL JEM-2000EX electron microscope. TEM graphs were taken after separating the surfactant from the metal particles by centrifugation. Typically 1 mL of the sample was centrifuged for 5 min at a speed of 14000 rpm. The upper part of the colorless solution was removed and the solid portion was redispersed in 1 mL of water. X-ray absorption spectra were recorded on beamline BL17C at the National Synchrotron Radiation Research Center (NSRRC) in Hsinchu, Taiwan.

EXAFS analyses were carried out using an analysis package, "REX" or "REX2000", coded by Rigaku. EXAFS oscillations [$\chi(k)$] were elucidated from the data by a spline smoothing method and normalized. The normalized k^3-weighted EXAFS spectra, $k^3\chi(k)$, were Fourier-transformed within k range from 2.5 to 13 $Å^{-1}$ to show the contribution of each bond pair in the Fourier transform (FT) peak. The experimental Fourier-filtered spectra were obtained from the inverse Fourier transformation with a Hanning window function in the r space range between 1.0 and 3.3 Å to determine the structural parameters for each bond pair. The structural parameters, such as the coordination number, the interatomic distance and the Debye-Waller factor, were used as adjustable parameters in the fitting process for the EXAFS spectra. The data were then analyzed by curve-fitting methods in k space using the following equation:

$$\chi(k) = \sum_i \frac{S_i N_i F_i(k_i) e^{-2\sigma_i^2 k_i^2}}{k_i r_i^2} \sin(2k_i r_i + \varphi_i(k_i))$$

$$k_i = \sqrt{k^2 - 2m_e \Delta E_i / \hbar^2}$$

where S_i, N_i, σ_i, and r_i, are an amplitude reduction factor, a coordination number, a Debye-Waller factor, and a bond distance for the i-th shell, respectively. $F_i(k)$ and $\varphi_i(k)$ are backscattering amplitude and a phase shift function, respectively. ΔE_i is the difference between the experimentally determined photoelectron kinetic energy (E_k) and absorption edge (E_0), which is used for theoretical calculations for phase shift and amplitude functions of the i-th shell. S_i was fixed at 0.8, which was obtained from the corresponding metal foil.

RESULTS AND DISCUSSION

Fig. 1 shows a typical TEM image of the gold nanoparticles and rods, indicating that the fusiform nanoparticles have been successfully synthesized as 0.2 mL(a) and 2 mL(b) growth solutions were added (Fig. 1). Compared to Figs. 1a and 1b, as the third (20 mL, Fig. 1c) growth solution was added, the nanorods could be observed; the average length was ~ 550 nm. The TEM analysis clearly indicates that the shape evolves from fusiform nanoparticles to 1-D rods. Note that the nanorods could be expanded up to 2 μm, and nanowires with the aspect ratios of up to 70 (Fig. 2a, the inset shows electron diffraction pattern of gold nanowires). Electron diffraction analysis of nanowires shows superpositions of a specific crystallographic zone corresponding to <110> and <111> zone of face-centered cubic structure, which was consistent with the previous study in nanorods synthesized via the CTAB system.[10] Sau and Murphy[13] established that amount and properties of seed particles critically determine the product. The diameter of seeds generally dictates the width of resulting product. This investigation develops a new method that keeps the [growth solution]/[seed] ratio constant through the reaction; the addition volume of growth solution is ten times that of the last addition. However, the length of rods cannot be extended by taking partial solution as seeds from one growth solution to the next one, because the [growth solution]/[seed] ratio increased with the further transfers, and seeds introduced into the system were too few to provide enough deposition sites. The rates of nucleation and growth are now widely believed to be dominated by the probabilities of collisions between several atoms, between atoms and clusters, and among two or more clusters. When only a few seeds were introduced into the growth solution, many atoms and a few seeds were present in the reaction system, and the probability of an effective collision between atoms exceeded the probabilities of the other two collisions. The collisions of atoms consume many atoms, which form nuclei, so the number of atoms grown on the surface of individual seeds dropped and tended to form small clusters. Consequently, the [growth solution]/[seed] ratio (volume) seemed to play the most important role in determining the final product; the evolution of shape strongly depends on the volume of growth solution added. The previous work with CTAB and gold nanorods suggested that during nanorod growth, preferential adsorption of CTAB to the different crystal faces of gold led to the inhibition of growth along the long axis of the rods and, therefore, enhanced growth at the ends of the nanorods.[15] It postulated at that time that CTAB bilayer formation would also encourage this anisotropic growth, in that CTAB molecules might

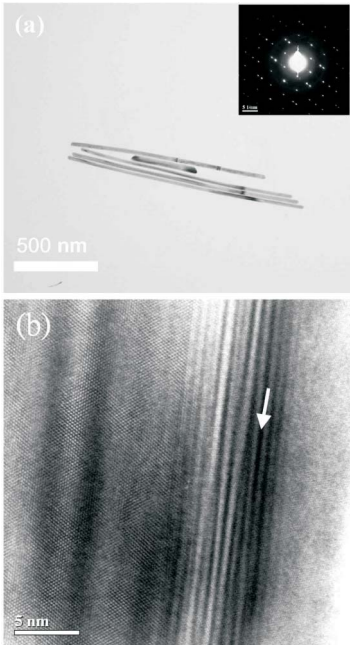

Fig. 2. TEM images of nanorods after the fifth growth solution (2000 mL) was introduced into the seed solution. The inset shows electron diffraction pattern of gold nanowires.

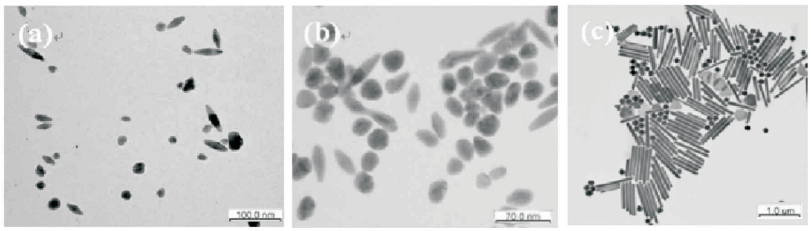

Fig. 1. TEM images of gold nanoparticles synthesized by this method. The A, B, C, and D represent the seed solutions after first (0.2 mL), second (2 mL), and third (20 mL) additions of growth solution, respectively.

have a preference for the side face of the rods via their headgroups and their tails would have a preference to interact with each other via van der Waals interactions. On the other hand, the effect of silver nitrate has been investigated, indicating that the branched gold particles were observed with the existence of silver nitrate.[3a,12] Nikoobakht and El-Sayed have proposed that silver ions could assist in the template elongation by pairing with Br^- ions of CTAB.[14] Nonetheless silver nitrate was essential for the formation of fusiform nanoparticles; some spherical or elliptic nanoparticles were observed without addition of silver nitrate (not shown). Therefore, the shape and length control has been achieved via varying the addition volume of growth solution.

X-ray absorption spectroscopy experiments were performed to provide better evidence of the oxidation state of gold nanoparticles throughout the reaction. Fig. 3 plots the X-ray absorption near edge structure (XANES) spectra of the Au L_3 edge over the reaction process. The absorption spectra of gold during the reaction can be distinguished, and the position depends on the oxidation state of gold. Notably, the spectrum before AA was added to (b) was consistent with the known Au^{3+} aqueous solution (a) and the position of absorption edge remained unchanged before AA was added, indicating that the redox reaction of gold ions does not occur in the surfactant aqueous solution. Following the addition of AA, the position of absorption edge significantly shifted to the same position as the Au foil. The color of the solution also turned from dark yellow to colorless immediately at the same time, which confirmed that AA reduced Au^{3+} ions to Au^0 atoms under the present condition. Generally gold nanocluster aqueous suspensions are believed to exhibit strong surface plasmon resonance peaks at ~ 530 nm, but the red color was not observed. This was because Au was present in isolated atoms, surrounded by surfactant molecules, rather than as nanoclusters formed by aggregation.

To obtain better evidence of the structural parameters of gold nanowires, EXAFS was performed. Fig. 4 shows the Fourier-transformed EXAFS spectra at the Au L_3-edge of gold foil and gold nanowires, respectively. In the case of the gold nanowires and gold foil, the main peak is attributed to the Au-Au metal bond. Just like in the corresponding foil case, the shape of the main peak was consistent with gold foil, indicating that the local structure of the as-prepared gold nanowire was similar to gold foil. Structural parameters (e.g., interatomic distance, coordination number, and Debye-Waller factor) for the gold foil and gold nanowires are obtained from EXAFS refinement (Table 1). This result suggests that the interatomic distance between the Au_{core} and the nearest neighboring Au atom is 2.86 Å which is consistent with the value for the bulk of gold (2.88 Å). The EXAFS data clearly confirms that gold nanowires prepared by our method are indeed of a face-centered cubic (fcc) phase of gold. Coordination number of gold nano-

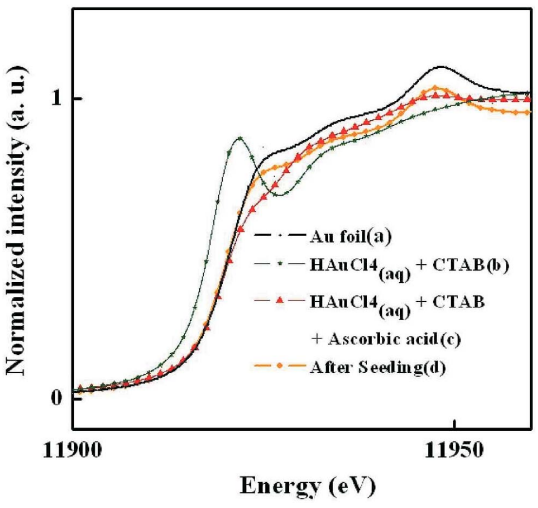

Fig. 3. X-ray absorption spectra of Au L_3 edge during the experiment. (a) Au foil. (b) the mixture of $HAuCl_4$ and CTAB solution. (c) after ascorbic acid was added. (d) after seeding.

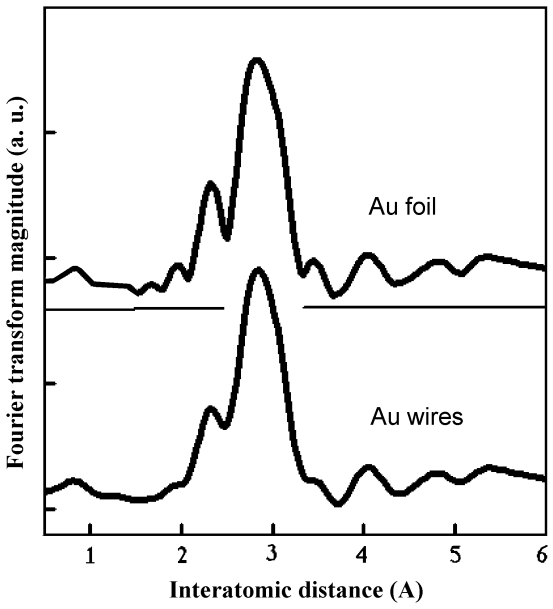

Fig. 4. Fourier-transformed EXAFS spectrum at the Au L_3-edge of the Au nanorods and Au foil.

Table 1. Curve-fitting analyses of EXAFS data for gold foil and gold nanowires

	Path	CN	R (Å)	σ^2 (Å^2)	ΔE (eV)
Foil	Au-Au	11.8(2)	2.88(2)	0.0065(7)	1.3(3)
Nanowires	Au-Au	11.0(3)	2.86(4)	0.015(2)	2.1(6)

wires was slightly smaller than that of gold foil; it was due to the nano-materials nature. As size of materials is reduced, increase of surface-to-volume ratio leads to the decrease of coordination number. It should be noted that the Debye-Waller factor of gold nanowire was significantly different from that of gold foil. In general, the Debye-Waller factor represents thermal disorder since every real system vibrates even at very low temperature due to zero-point energy. The Debye-Waller factor is given by $\sigma^2 = \sigma_{vib}^2 + \sigma_{stat}^2$ where σ_{vib} and σ_{stat} are the vibrational and static disorders, respectively.[23] Usually the absolute of the Debye-Waller factor between the standard and unknown compounds is important. The refinement result shows that the Debye-Waller factor of gold nanowires was greatly larger than that of gold foil, which implies that there were some structural defects in the local structure. The twin defects have been observed in the result of HRTEM, which was consisted with the result of EXAFS refinement. These structural defects were usually obtained in nano-materials because of the "bottom up" synthesis process. On the other hand, the surface nature of seed particles plays an important role in this synthesis process. Surface facets of seed particles determine the shape of the resulting product, and zeta potential (surface charge) results in the aspect ratio of nanorods.[24] Besides the abovementioned factors, several reaction parameters also determined the shape and aspect ratio of the resulting product, including size of seed particles, reaction temperature, crystallinity of seed particles, and concentration of seed solution. A number of synthesized factors have influence on the product, and some structural defects were formed easily. Thus the structural parameters have been analyzed.

CONCLUSIONS

The TEM images show the change in the morphology of gold nano particles during the reaction: the shape of the gold nanoparticles evolved from fusiform into 1-D rods as more growth solution was added. By using XAS, we have experimentally elucidated a growth mechanism for 1-D gold nanorods via this method. XANES spectra of the Au L_3 edge monitors the change in the valence of gold, indicating AA can reduce the gold ions to atoms at room temperature. EXAFS spectra clearly confirm the environment around gold atoms over the reaction and the growth of Au nanorods. Accordingly, a simple route for the large-scale synthesis of 1-D nanorods of gold, whose length and shape is controllable by varying the amount of growth solution, was demonstrated. These particles are expected to have wide applications in sensing and other related fields.

ACKNOWLEDGMENT

We would like to thank the National Science Council of the Republic of China, Taiwan, for financially supporting this research under Contract No. NSC 94-2113-M-002-030. We also thank the Industrial Technology Research Institute for financial support.

Received June 13, 2006.

REFERENCES

1. (a) Murphy, C. J. *Science* **2002**, *298*, 2139. (b) Hu, J.; Odom, T. W.; Lieber, C. M. *Acc. Chem. Res*. **1999**, *32*, 435. (c) El-Sayed, M. A. *Acc. Chem. Res*. **2001**, *34*, 257. (d) Huang, M. H.; Mao, S.; Feick, H.; Yan, H.; Wu, Y.; Kind, H.;Weber, E.; Russo, R.; Yang, P. *Science* **2001**, *292*, 1897. (e) Huynh, W. U.; Dittmer, J. J.; Alivisatos, A. P. *Science* **2002**, *295*, 2425.
2. (a) Yu, Y.-Y.; Chang, S.-S.; Lee, C.-L.; Wang, C. R. Chris. *J. Phys. Chem. B* **1997**, *101*, 6661. (b) Wilson, O.; Wilson, G. J.; Mulvaney, P. *Adv. Mater.* **2002**, *14*, 1000. (c) Favier, F.; Walter, E.; Zach, M. P.; Benter, T.; Penner, R. M. *Science* **2001**, *293*, 2227. (d) Maier, S. A.; Kik, P. G.; Atwater, H. A.; Meltzer, S.; Harel, E.; Koel, B. E.; Requicha, A. A. G. *Nat. Mater.* **2003**, *2*, 229.
3. (a) Jana, N. R.; Gearheart, L.; Murphy, C. J. *Adv. Mater.* **2001**, *13*, 1389. (b) Jana, N. R.; Gearheart, L.; Murphy, C. J. *J. Phys. Chem. B* **2001**, *105*, 4065.
4. Esumi, K.; Keiichi, K.; Torigoe, K. *Langmuir* **1995**, *11*, 3285.
5. Ahmadi, T. S.; Wang, Z. L.; Green, T. C.; Henglein, A.; El-Sayed, M. A. *Science* **1996**, *272*, 1924.
6. Sun, Y.; Gates, B.; Mayers, B.; Xia, Y. *Nano Lett.* **2002**, *2*, 165.

7. Jr, M. B.; Moronne, M.; Gin, P.; Weiss, S.; Alivisatos, A. P. *Science* **1998**, *281*, 2013.
8. Murphy, C. J.; Jana, N. R. *Adv. Mater.* **2002**, *14*, 80.
9. Chang, S.-S.; Shih, C.-W.; Chen, C.-D.; Lai, W.-C.; Wang, C. R. Chris. *J. Phys. Chem. B* **1999**, *15*, 701.
10. Johnson, C. J.; Dujardin, E.; Davis, S. A.; Murphy, C. J.; Mann, S. *J. Mater. Chem.* **2002**, *12*, 1765.
11. Busbee, B. D.; Obare, S. O.; Murphy, C. J. *Adv. Mater.* **2003**, *15*, 414.
12. Sau, T. K.; Murphy, C. J. *J. Am. Chem. Soc.* **2004**, *126*, 8648.
13. Sau, T. K.; Murphy, C. J. *Langmuir* **2004**, *20*, 6414.
14. Nikoobakht, B.; El-Sayed, M. A. *Chem. Mater.* **2003**, *15*, 1957.
15. Gao, J.; Bender, C. M.; Murphy, C. J. *Langmuir* **2003**, *19*, 9065.
16. Tornblom, M.; Henriksson, U. *J. Phys. Chem. B* **1997**, *101*, 6028.
17. Chen, H. M.; Peng, H. C.; Liu, R. S.; Asakura, K.; Lee, C. L.; Lee, J.-F.; Hu, S. F. *J. Phys. Chem. B* **2005**, *109*, 19553.
18. Chen, H. M.; Peng, H. C.; Liu, R. S.; Hu, S. F.; Jang, L.-Y. *Chem. Phys. Lett.* **2006**, *420*, 484.
19. Chen, H. M.; Liu, R. S.; Jang, L.-Y.; Lee, J.-F.; Hu, S. F. *Chem. Phys. Lett.* **2006**, *421*, 118.
20. Toshima, N.; Harada, M.; Yonezawa, T.; Kushihashi, T.; Asakura, K. *J. Phys. Chem.* **1991**, *95*, 7448.
21. Harada, M.; Asakura, K.; Ueki, Y.; Toshima, N. *J. Phys. Chem.* **1992**, *96*, 9730.
22. Toshima, N.; Harada, M.; Yamazaki, Y.; Asakura, K. *J. Phys. Chem.* **1992**, *96*, 9927.
23. Iwasawa, Y. *X-ray Absorption Fine Structure for Catalysts and Surfaces*; World Scientific: Singapore, 1996.
24. Gole, A.; Murphy, C. J. *Chem. Mater.* **2004**, *16*, 3633.